AD-A120 065 CALIFORNIA UNIV LOS ANGELES DEPT OF MATERIALS SCIEN--ETC F/G 11/6
ACOUSTIC EMISSION BEHAVIOR OF NICKEL DURING TENSILE DEFORMATION--ETC(U)
SEP 82 S S HSU, K ONO N00014-81-K-0011
UNCLASSIFIED TR-82-02 NL

SECURITY CLASSIFICATION OF THIS PAGE (When Data Entered)

| REPORT DOCUMENTATION PAGE | READ INSTRUCTIONS BEFORE COMPLETING FORM |
|---|---|
| 1. REPORT NUMBER: TR-82-02 (12) 2. GOVT ACCESSION NO.: AD-A120 065 | 3. RECIPIENT'S CATALOG NUMBER |
| 4. TITLE (and Subtitle): Acoustic Emission Behavior of Nickel during Tensile Deformation | 5. TYPE OF REPORT & PERIOD COVERED: Technical |
| | 6. PERFORMING ORG. REPORT NUMBER |
| 7. AUTHOR(s): S.-Y. S. Hsu and K. Ono | 8. CONTRACT OR GRANT NUMBER(s): N00014-81-K-0011 |
| 9. PERFORMING ORGANIZATION NAME AND ADDRESS: University of California, Los Angeles, California 90024 | 10. PROGRAM ELEMENT, PROJECT, TASK AREA & WORK UNIT NUMBERS |
| 11. CONTROLLING OFFICE NAME AND ADDRESS: Physics Program, Physical Sciences Div., Office of Naval Research, Arlington, Virginia 22217 | 12. REPORT DATE: September 1982<br>13. NUMBER OF PAGES: 9 |
| 14. MONITORING AGENCY NAME & ADDRESS (if different from Controlling Office): Office of Naval Research Branch Office, 1030 East Green Street, Pasadena, California 91101 | 15. SECURITY CLASS. (of this report): Unclassified<br>15a. DECLASSIFICATION/DOWNGRADING SCHEDULE |

16. DISTRIBUTION STATEMENT (of this Report)

Approved for public release, distribution unlimited



17. DISTRIBUTION STATEMENT (of the abstract entered in Block 20, if different from Report)

18. SUPPLEMENTARY NOTES

To be published in The Proceedings of the 6th International Acoustic Emission Symposium, Susono City, Japan, 31 October - 3 November 1982.

19. KEY WORDS (Continue on reverse side if necessary and identify by block number)

Acoustic Emission
Nickel
Plastic deformation
Quench aging

20. ABSTRACT (Continue on reverse side if necessary and identify by block number)

see next page

DD FORM 1 JAN 73 1473 EDITION OF 1 NOV 65 IS OBSOLETE
S/N 0102-LF-014-6601

SECURITY CLASSIFICATION OF THIS PAGE (When Data Entered)

# ACOUSTIC EMISSION BEHAVIOR OF NICKEL DURING TENSILE DEFORMATION

S.-Y. S. Hsu* and K. Ono
Materials Science and Engineering Department
School of Engineering and Applied Science
University of California
Los Angeles, Calif. 90024

* Now at Dunegan/Endevco, San Juan Capistrano, CA

## Abstract

Commercial 99.6% purity nickel (Ni-200) was studied in detail for its AE behavior. The specimens slowly cooled from high-annealing temperature exhibited much higher AE signal levels than the quenched samples. This was attributed to the existence of solute pinning atmospheres around dislocations. The kinetic study using AE technique quantitatively determined the activation energy of solute diffusion, which was found to be close to the activation energy for the carbon diffusion in nickel. An AE source model based on the dislocation acceleration and/or deceleration following unpinning was presented. The effects of deformation temperature, including dynamic strain aging phenomenon, were also discussed.

## INTRODUCTION

With the combined features of high sensitivity and dynamic nature, Acoustic Emission (AE) technique is a useful tool for the study of plastic deformation behavior because signals generated by dislocation motions can be detected. Numerous factors which affect the dislocation movements have been examined by AE, including the effects of crystal structures, grain size, second phase particles, stacking fault energy, and solute concentration (1-3). The effect of solute atom segregation, known to be an important factor on dislocation behavior, has also been detected by AE during initial yielding and serrated yielding process (4), but no detailed study of the extent of segregation on AE has been reported. The purpose of this study is to investigate more systematically the effect of solute segregation on the AE behavior of materials.

It has been established experimentally that interstitial elements can cause serrated yielding and strain aging effect in nickel. Sukhovarov (5) noted serrated yielding in a temperature range around 200°C. The effect disappeared after a wet hydrogen anneal. It was thus attributed to carbon and/or nitrogen interstitials. Subsequent kinetic studies (6,7) deduced an activation energy of 125 KJ/mole (30 Kcal/mole), roughly equal to the activation energy for the diffusion of carbon in nickel (150 KJ/mole or 35.7 Kcal/mole). Blakemore (8) confirmed that nitrogen charged nickel does not show strain aging effects while nickel-carbon does. A recent study of Ni (carbon content of 0.1%) gave an activation energy of 104 KJ/mole (25 Kcal/mole), and the aging phenomena were attributed to the interaction between carbon vacancy pairs and dislocations (9).

Therefore, in this study, commercial purity Ni-200 specimens were studied in detail through different testing temperatures and different heat treatment conditions to determine the influences of impurities on AE behavior. Since nickel also has a high stacking fault energy and has a similar overall dislocation behavior to that in aluminum, the comparison of AE behavior between Ni

and high pure Al (99.99%) reported in our previous study [10] will further clarify the effects of solute atoms in AE behavior.

## MATERIALS AND EXPERIMENTS

An annealed 3.18mm (0.125") thickness Ni-200 sheet was purchased from Huntington Alloy Co. The chemical composition indicated 0.02% Si, 0.01% Fe, 0.01% C, 0.24% Mn and 0.05% C. As-received material was cold-rolled to 1.3mm (0.05") thickness before machining.

Two types of specimen geometries were prepared: the large size specimens were used for investigating the effects of deformation temperature. It has an overall size of 305mm x 25mm (12" x 1"), and the gage section is 32mm (1.25") long and 6.4mm (0.25") wide. The small size specimens were used for studying heat treatment effects and aging kinetics. The overall size of these specimens is 152mm x 20mm (6" x 0.8") with the gage section reduced to 2.5mm x 5.1mm (1" x 0.2"). After machining, all specimens were heat treated. Large specimens used for the study of deformation temperature effect were annealed at 1073K for 1 hr., followed by slow furnace cool. The final grain size was about 43 m. Small size specimens were heat treated differently according to the purpose of the test. These heat treatments will be described in the next section. The samples were loaded in an Instron using a pair of pin loading grips. Before a test, the holes for loading pins were prestressed to minimize friction noises.

The setup for tensile testing and AE detection was the same as that for pure metals described in the previous paper (10). Basically, a 100 kHz PZT element was attached to one end of a waveguide, which was soldered to a sample. The output was amplified and the intensity was monitored using a true-rms voltmeter. The nominal strain rate of the tensile test was $7 \times 10^{-4}$/s.

## RESULTS

Figure 1 plots the change of strengths with deformation temperatures. Initial discontinuous yielding existed at temperatures below 673K and serrated yielding appeared between 473K and 673K. The work-hardening rate remained high up to 673K, resulting in nearly constant tensile strength between 300K and 573K. Above 573K tensile strength dropped at faster rates with increasing temperatures. These observations suggest the existence of dynamic strain aging effects through the process of solute atom pinning and unpinning of dislocations at temperatures below 673K.

The rms voltage of AE signals ($V_r$) vs. strain curve of the well-annealed specimen deformed at 300K is shown in Fig. 2. The characteristics of this AE behavior were typically observed in other Ni specimens tested below 673K and were quite different from that of Al and Cu previously reported (10). These include:

1) AE signal level is about 10 times higher than that in Al and Cu when the peak AE output near macroscopic yielding is compared.
2) $V_r$ near macroscopic yielding is not smooth; instead, it contains numerous large spikes due to burst-type signals.
3) After the initial peak, AE signal level drops sharply to about one-fourth of the peak value, in contrast to the gradual decrease observed in Al and Cu.
4) Following the sharp decrease, the average AE level remains nearly unchanged up to 30% plastic strain and many excursions of $V_r$ level are superposed.

Also shown in Fig. 2 is the $V_r$-strain curve of the specimen quenched from 1073K. The peak AE output is only 30 mV (with 60dB amplification) and no fluctuations of $V_r$ during deformation were observed. This is the typical $V_r$-strain curve observed in pure Al or Cu (10), and the differences in AE behavior between quenched and slowly cooled specimens are evident.

The variation of $V_r$-strain curves with deformation temperature is equally significant as with cooling rate effect. Fluctuations of $V_r$ below 673K were basically continuous signals in nature, and the amplitude of such fluctuations increased with temperature. At 673K, large spikes were repeatedly detected between 15 and 30% plastic strain. At 773K, fluctuations vanished completely, but peak AE output near macroscopic yielding was still high. AE behavior returned to the typical character-istics observed in pure Al at 873K, which was also similar to that of the quenched specimen in Fig. 2. The variation of peak AE level with temperature is also shown in Fig. 1. The peak AE level reached a maximum at about 650K or 0.38 $T_m$ ($T_m$ is the absolute melting temperature of Ni). This fell into the same homologous temperature ranges where the maximum AE levels were reached in Al and Cu.

In order to identify any effect from interstitial solute atoms, a series of tests were conducted on small size specimens, which received different heat treatments. These specimens were first water-quenched from 1073K after annealing at that temperature for 0.5 hr. They were subsequently annealed at lower temperatures (373K to 673K) for a period of 200 minutes, followed by water-quenching. The yield strengths and peak AE output levels of these tests were plotted in Fig. 3 as functions of annealing temperature. Quenching from 1073K (as quenched) resulted in low AE output levels and smooth $V_r$-strain curves, as shown in Fig. 2. With an increase of annealing temperature from 300K to 573K, the peak AE level increased almost ten times and the $V_r$-strain curve regained the characteristics of slow-cooled specimens shown in Fig. 2. With a further increase in the annealing temperature to 673K, however, the AE characteristics were almost identical to that from as-quenched one.

The results in Fig. 3 strongly suggest the possibility of forming solute pinning atmospheres around dislocations in this material. To further identify the mechanism of the formation of pinning atmosphere, a kinetic study was carried out to obtain the activation energy of diffusing species. As-quenched specimens (1073K, 0.5 hr) were annealed at 473K, 493K, 508K and 523K for different periods of time (5 to 200 mins.), followed by water-quenching. The peak AE level vs. annealing time at different annealing temperatures were evaluated. These curves closely resemble the strain aging phenomenon in mild steels where interstitial carbon locking mechanism is the basic cause. For impurity diffusion to the core of an edge dislocation, Cottrell and Bilby (11) calculated the rate of accumulation. The number of solute atoms removed from solution after time t at temperature T is given by:

$$C_t = 3L(\pi/2)^{1/2} C_o[ADt/kT]^{2/3} \qquad (1)$$

where $C_o$ is the initial concentration of the solute atoms, A is a constant, L is the dislocation density, and D is the diffusion coefficient of the solute atom at temperature T, respectively. This relationship is valid for the early stages of segregation only. Harper (12) proposed a simple generalization to fit later stages by assuming that the rate of flow is decreased in proportion with the amount already segregated. He obtained:

$$C_t = 1 - \exp[-3L(\pi/2)^{1/2} (ADt/kT)^{2/3}] \qquad (2)$$

and tested this relationship experimentally in iron-carbon and iron-nitrogen alloys. Good agreements were observed between the prediction and the experimental results. Similar dependence has been observed in nickel-hydrogen

alloys (13). Following the procedures of Harper, we plotted log(1-f) against $t^{2/3}$ in Fig. 4. Here, f is the fractional variation of the peak AE level and is given by

$$f = \frac{V_r - V_{r,min}}{V_{r,max} - V_{r,min}} \qquad (3)$$

$V_{r,max}$ is the maximum level of $V_r$ and $V_{r,min}$ correspond to the minimum value. From experiment, $V_{r,max}$ = 260$\mu$V and $V_{r,min}$ = 30 $\mu$V were obtained. A good linear relationship is shown at all four temperatures. This clearly indicates the kinetics to be that of Cottrell-Bilby-Harper theory. When the values of ln(T/t) are plotted against the inverse of the absolute temperature for the case of log(1-f) = - 0.2, the slope of this line gives the activation energy Q of 138 KJ/mole (33.0 Kcal/mole). This is in good agreement with the activation energy for diffusion of carbon in nickel (34 to 36 Kcal/mole) (14,15). Thus, we may conclude the annealing effect in quenched Ni to be due to carbon diffusion to dislocations.

## DISCUSSION

The major experimental findings are summarized in the following:

1) Specimens quenched from temperatures between 1073K and 673K exhibit the characteristic AE behavior of pure Al and Cu when tested at room temperature.
2) Specimens quenched from temperatures below 673K or those slow-cooled possess distinct AE characteristics significantly different from those in Al or Cu; that is, higher peak AE levels, many spikes in the $V_r$-strain curve upon yielding, rapid drop in the signal levels after yielding and many fluctuations in $V_r$ the work-hardening region.
3) The kinetics for the appearance of high AE output levels are controlled by carbon diffusion to dislocations.
4) For slow-cooled specimens, the temperature corresponding to maximum peak AE output, $T_c$, is about 0.38 $T_m$, which is in the same homologous temperature range as that of Al and Cu.

### AE Behavior in Quenched Nickel

The AE response of nickel quenched from temperatures at 673K and above displayed a simple $V_r$-strain curve with a peak AE output level comparable to that in high purity Al or Cu. Effects from quenched-in vacancies and thermal stress introduced by the quenching process should depend strongly on the quenched temperature. Because of the observed independence of AE behavior on the quenching temperature above 673K, the quenched-in vacancies and thermal stress are believed to have no effect on AE behavior.

Published electron microscopy works on Ni indicated the similarities in over-all dislocation substructures among Al, Cu and Ni. For example, Swann (16) observed the structures in Ni deformed at moderate temperature (510K) to be characterized by a cell structure with relatively sharp walls and cell interiors containing few dislocations. In contrast, Ni deformed at low temperature (77K) showed the cell walls to be not as distinct as those at 510K, and in most regions the interior of the cell contained scattered dislocations (17). The stacking fault energy of Ni, although still rather poorly defined, is higher than 100 mJ/m$^2$ (18). A commonly assumed value is 120 mJ/m$^2$ (19), which is between the SFE of Al (= 200 mJ/m$^2$) and Cu (= 50 mJ/m$^2$). Thus, the dislocation glide behavior of Ni is expected to be similar to that in Al or Cu. This should produce similar AE behavior among these three

materials if impurities contained in nickel are not involved.

The nickel samples used in this study were less pure (99.6%) than Al and Cu (both 99.9% or better) (10). Interstitial impurity atoms, such as carbon and hydrogen, have been found to pin dislocations in nickel (9). However, it has been shown that such pinning effect disappears above 573K. For example, serrations in Ni-C alloys were observed (20) over the temperature range of 223K to 573K, and a peak in the flow stress of nickel containing carbon has been reported at 473K (5). For Ni-H system, the serrated flow was observed between 253K to 153K (13), while the static strain aging effect was shown between 323K to 573K (21). Accordingly, pinning effects from impurities are not expected to be signif icant in samples quenched from temperatures above 573K. Combined with the observations in dislocation substructures, we should expect the similar AE beha vior between Al, Cu, and the nickel samples quenched from 673K and above. Such expectation agrees with the experimental findings.

AE Behavior in Slow-Cooled Nickel Samples

The AE characteristics detected in the slow-cooled nickel samples were distinctly different from those in quenched ones. The kinetic study given in the last section has indicated that the rate-controlling mechanism for the transition of AE characteristics from quenched type to slow-cooled type is the carbon diffusion to dislocations. The major effect for the carbon segregation is to form Cottrell atmosphere around dislocations. Such an increase of carbon concentration around dislocations will proportionally increase the stress needed to break the dislocation away from pinning atmospheres and decrease greatly the number of initial mobile dislocations. When the unlocking stress is approached under tensile loading, both dislocation unpinning and dislocation multiplication will take place. In the following we will discuss how such unpinning and multiplication process can produce the peculiar AE behavior observed in the slow-cooled specimen.

Following Malen and Bolin (22), Ono (23) and Landy and Ono (24) derived the maximum of the stress pulse ($\sigma_{max}$) generated when inelastic strain is created during the acceleration or deceleration of a mobile dislocation:

$$\sigma_{max} \propto S_m/\tau^2 \qquad (4)$$

where $S_m$ is proportional to the localized plastic srain increment, $\Delta\epsilon^*$, and $\tau$ is defined as the risetime of the event. For the stress wave generated by a moving dislocation segment with the length L and the distance moved x, Eq. (4) becomes

$$\sigma_{max} \propto L\,\Delta x/\tau^2. \qquad (5)$$

The transducer reponse to such a wave pulse is (25)

$$R^{max} = C\,L\,\Delta x/\tau \qquad (6)$$

where $R^{max}$ is the peak voltage of the transducer response, and C is a constant. It should be emphasized here that the $\Delta x$ value only takes into account the non-equilibrium dislocation motion, i.e., when undergoing acceleration or deceleration. For continuous signals due to a large number of dislocation motion within the volume without any spatial or time correlation, the rms voltage output from the transducer $V_r$ is given by

$$V_r = C\sqrt{\dot{N}}\,L\,\Delta x/\tau \qquad (7)$$

where $\dot{N}$ is the event rate, that is, the number of stress waves exciting the

transducer per unit time.

To interpret the unpinning process with this model, consider a simplified pinning atmosphere with a square-well force-displacement curve as the interaction force between pinning points and dislocations. Figure 5 illustrates such a force-distance curve of the atmosphere. Under the imposed deformation rate, the stress acting on a potentially mobile dislocation increases initially. At time t = 0, the localized stress reaches $\sigma_o$, a necessary stress level to break dislocations away from pinning points without thermal assistance. Once breakaway occurs, an unbalanced force exits which would cause dislocation acceleration to its terminal velocity. The equation of motion for t > 0 is given by

$$\sigma_o b = m^* (dV/dt) + B V \qquad (8)$$

where $m^*$ is the effective mass per unit length of the dislocation line and B is the drag coefficient. Under the following conditions:

$$V = 0 \text{ at } t = 0 \quad \text{and} \quad V = \sigma_o b/B \text{ at } t \to \infty,$$

the dislocation velocity V can be obtained. The event risetime may be defined as the time period dislocation reaches 90% of its terminal velocity, and $\Delta x$ is the distance dislocation moved between t = 0 and $t = 4\tau$. Using Eq. (8), we obtain the following expression for the transducer output level due to the breakaway of a dislocation segment length L:

$$V_r \alpha \sqrt{N}\, L\, \sigma_o b/B. \qquad (9)$$

This equation indicates that, when the strongly pinned dislocations in the slow-cooled specimen are unlocked, large acceleration due to large unbalanced force can generate strong AE signals. Furthermore, because most of the potentially mobile dislocations were pinned initially, high unpinning rate occurs once $\sigma_o$ is reached. This would give high event rate N, contributing to higher transducer output voltage $V_r$.

Equation (9) may also be used to explain the high AE output from dislocation multiplication by considering the operation of Frank-Read sources. Here, $\sigma_o$ can be considered as the critical stress for the source operation at which a dislocation loop can detach from the source and accelerates away. However, the risetime for this process is expected to be greater than the unpinning, resulting in the lower AE levels. This is why the observed AE levels are higher with the presence of solute segregation.

Dynamic Strain Aging Effect

Another AE characteristic which distinguishes the slow-cooled nickel samples from the quenched ones is the presence of AE fluctuations during work hardening. Such fluctuations existed in the slow-cooled samples during high temperature deformation up to 673K. In the load-elongation curves, serrations of stress levels were observed at 473K, 573K and 673K. Both perturbations were found to appear at the same strain and the magnitude. At 773K and 873K, however, both the load serrations and AE fluctuations disappeared completely. It is therefore reasonable to conclude that both stress serrations and AE fluctuations during deformation have the same origin.

Because the AE fluctuations occurred repeatedly at a high rate during deformation, it is difficult to analyze the relationship between AE fluctuations and stress serrations of nickel in detail. However, the interpretations on the dynamic strain aging (DSA) phenomenon can be used to explain the general features of AE fluctuation, based on the previous discussions of the AE source mechanisms. When the solute dragging force is overcome by the

increase of stress level, localized yielding occurs. Dislocations either are unpinned from solute atmospheres, or rapid multiplication processes, leading to the increase of AE output levels. This is quite similar to that observed during initial yielding, except that the extent of such localized yielding is smaller during DSA. Once unpinning or rapid multiplication occurs, stress level reduces to accommodate the imposed strain rate, and the AE output level returns to the average level because those newly generated dislocations are rapidly immobilized due to dislocation-dislocation interactions. It was noticed that the amplitude of AE fluctuations increased when the deformation temperature was raised from 300K to 673K. This increase reflects the change of the solute drag force, although in stress-strain curves, the change in the extent of serrations is not obvious.

## CONCLUSIONS

This study demonstrates the usefulness of AE technique for the study of plastic deformation behavior. Through its AE signatures, the effect of solute pinning on dislocation dynamics is clearly discernible and the extent of solute segregation can be studied quantitatively. The AE characteristics of nickel are:

1) For specimens without solute pinning atmospheres, i.e., interstitial solute atoms were randomly distributed, the AE characteristics were similar to those observed in pure Al or Cu.
2) With the formation of pinning atmosphere, distinct AE features were detected. These include higher peak AE levels, many spikes in the $V_r$-strain curve upon yielding, rapid drop in the signal level after yielding, and many fluctuations in the work-hardening region.
3) The kinetics for the appearance of high AE output levels were controlled by the carbon diffusion to dislocations.

An AE source model, which is based on the theory of elastic wave radiation through dislocation acceleration and/or deceleration was presented. This model takes into account the sensor response to continuous type signals and qualitatively explains the increase of AE signal level due to solute pinning effect.

## ACKNOWLEDGEMENTS

We are grateful for the support of this research by the U. S. Office of Naval Research, Physics Program.

## REFERENCES

1. S.H. Carpenter and C.R. Heiple (1979) Fundamentals of Acoustic Emission, ed., K. Ono, University of California, Los Angeles, p. 49.
2. T. Kishi and K. Kuribayashi (1979) Fundamentals of Acoustic Emission," ed, K. Ono, University of California, Los Angeles, p. 105.
3. C. Scruby, H.N.G. Wadley and J.Speake (1980) Int. Metals Rev., Review 249 25, 41-64.
4. J. Eisenblatter, P. Jax and H.J. Schwabe (1974) The Second Acoustic Emission Symposium, Tokyo, Japan, September, Session 7, 1.
5. V. Sukhovarov (1962) Phys. Met. Metall., 13(2), 109.
6. V. Sukhovarov, N.A. Aleksandrov and L.A. Kudryavtseva (1962) Phys. Met. Metall., 14(6), 82.
7. L. Popov and V. Sukhovarov (1964) Phys. Met. Metall., 17(3), 428.
8. J. Blakemore (1968) Ph.D. Thesis, University of Newcastle, Newcastle, U.K.
9. W.R. Cribb and R.E. Reed-Hill (1977) Met. Trans. 8A, 71.

10. S.-Y. S. Hsu and K. Ono (1980) The Fifth Acoustic Emission Symposium, Jpn.Soc.NDI, Tokyo, Japan, Session 7, p. 283, November.
11. A.H. Cottrell and B.A. Bilby (1949) Proc. Phys. Soc. A62, 49.
12. S. Harper (1951) Phys. Rev. 83, 709.
13. T. Boniszewski and G.C. Smith (1963) Acta Met., 11, 165.
14. I.I. Kovenski (1963) Phys. et Metall., 16, 613.
15. S. Diamond and C. Wert (1967) Trans. AIME, 239, 705.
16. P.R. Swann (1963) Electron Microscopy and Strength of Crystals," eds. G. Thomas and J. Washburn, Interscience, New York, p. 131.
17. W.P. Longo and R.E. Reed-Hill (1974) Metallography, 7, 181.
18. P.J.C. Gallagher (1970) Met. Trans., 11, 2429.
19. R.J. McElory and Z.C. Szkopiak (1972) Int. Met. Review, 17, 175.
20. Y. Nakada and A.S. Keh (1970) Acta Met., 18, 437.
21. E. Macheraugh and O. Vohringer (1963) Acta Met.,11, 157.
22. K. Malen and L. Bolin (1974) phys. stat. sol(B), 61, 637.
23. K. Ono (1979) Fundamentals of Acoustic Emission ed., K. Ono, University of California, Los Angeles, p. 167.
24. R.J. Landy and K. Ono (1982) J. Acoust. Emission, 1, 7-19.

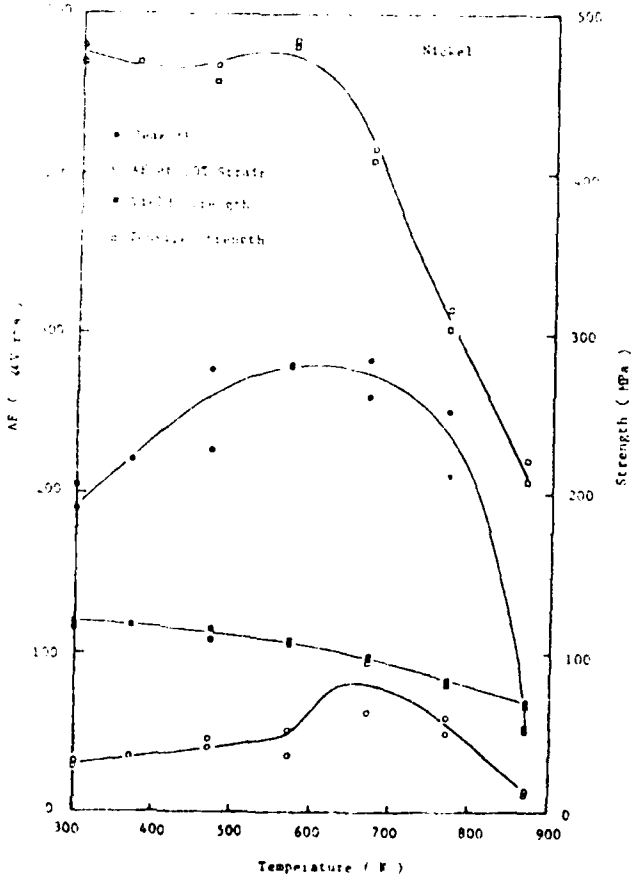


Fig. 1 The effects of deformation temperature on the AE output levels and mechanical properties of slow-cooled nickel.

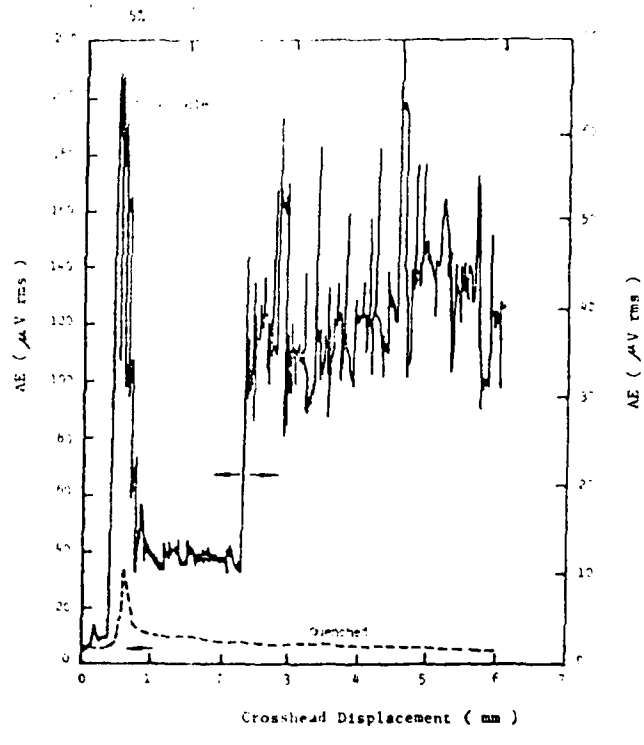


Fig. 2 The characteristics of AE vs. displacement of nickel under slow-cooled (solid line) and quenched (dashed line) conditions.

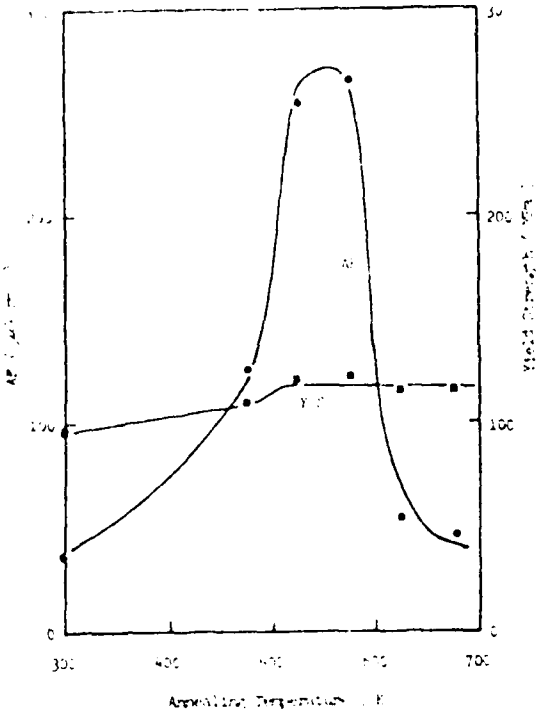

Fig. 3 The effect of annealing temperature on the peak AE output levels and yield strength of nickel quenched from 1073K.

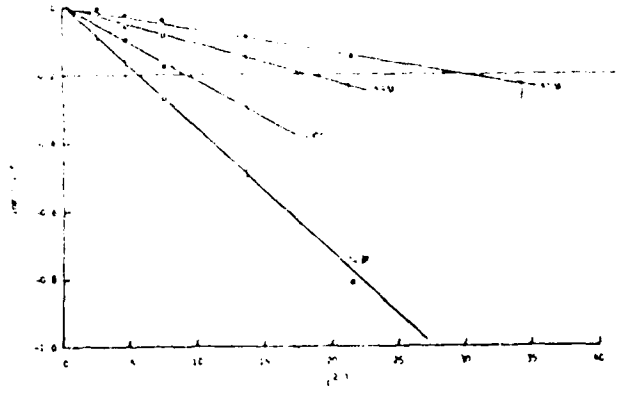

Fig. 4 log(1-f) vs $t^{2/3}$ plot indicating the effect of annealing temperature on the rate of AE increase in nickel.

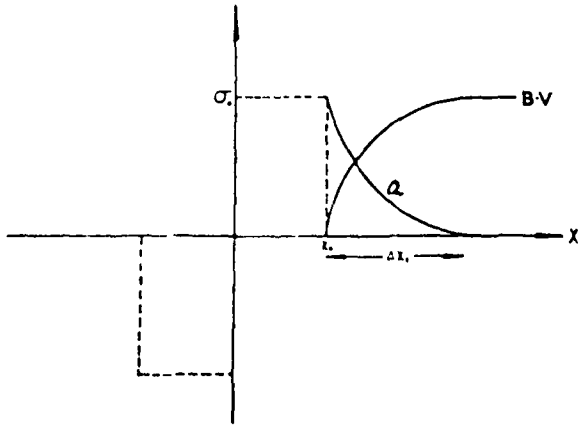


Fig. 5 A schematic diagram for the initiation of dislocation motion.
$\sigma_i$: unbalanced stress;
a: dislocation deceleration;
B: drag coefficient;
V: dislocation velocity.
Dash lines represent the stress field of pinning atmospheres.

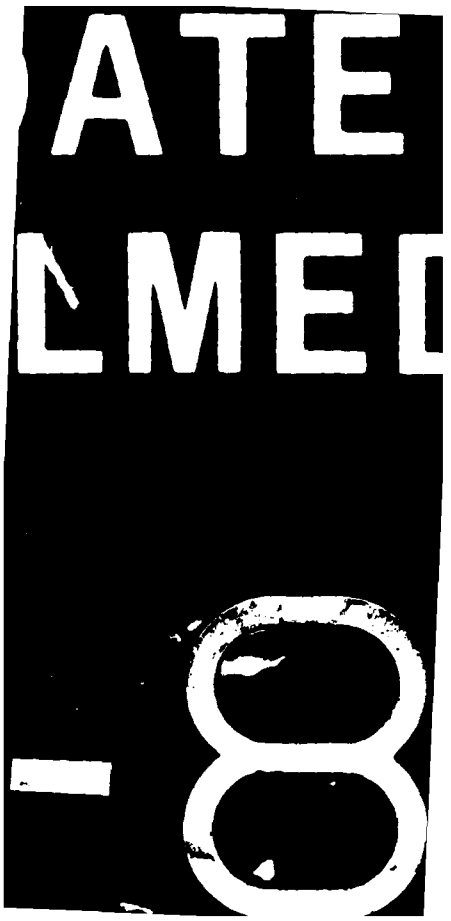
ATE
LMED
8